Targher Giovanni (Orcid ID: 0000-0002-4325-3900)
Byrne Christopher D (Orcid ID: 0000-0001-6322-7753)
Zheng Ming-Hua (Orcid ID: 0000-0003-4984-2631)
Geng Bin (Orcid ID: 0000-0001-7573-8710)

Hepatocellular Cystathionine γ lyase/Hydrogen sulfide Attenuates Non-Alcoholic Fatty Liver Disease by Activating Farnesoid X Receptor

Wenjing Xu[1†], **Changting Cui**[2†], Chunmei Cui[3], Zhenzhen Chen[2], Haizeng Zhang[2], Qinghua Cui[3], Guoheng Xu[3], Jianglin Fan[1], Yu Han[4], Liangjie Tang[6], Giovanni Targher[6], Christopher D. Byrne[7], Ming-Hua Zheng[4,5*] Liming Yang[8*], Jun Cai[2*], Bin Geng[2*]

1. Department of Pathology, School of Basic Medical Science, Xi'an Medical University, Shanxi, China
2. Hypertension Center, State Key Laboratory of Cardiovascular Disease, National Center for Cardiovascular Diseases, Fuwai Hospital of Chinese Academy of Medical Sciences and Peking Union Medical College, Beijing, China
3. Department of Bioinformatics, Physiology and Pathophysiology, School of Basic Medical Sciences, Peking University, Beijing China
4. NAFLD Research Center, Department of Hepatology, the First Affiliated Hospital of Wenzhou Medical University; the Key Laboratory of Diagnosis and Treatment for the Development of Chronic Liver Disease in Zhejiang Province, Wenzhou, China
5. Department of Gastrointestinal Surgery, the First Affiliated Hospital of Wenzhou Medical University, Wenzhou, China
6. Section of Endocrinology, Diabetes and Metabolism, Department of Medicine, University and Azienda Ospedaliera Universitaria Integrata of Verona, Verona, Italy
7. Southampton National Institute for Health and Care Research Biomedical Research Centre, University Hospital Southampton, Southampton General Hospital, Southampton, UK
8. Department of Pathophysiology, Harbin Medical University-Daqing, Daqing, China.

Keywords
Cystathionine γ lyase
Hydrogen Sulfide
Non-alcoholic fatty liver
Farnesoid X receptor
Sulfhydration

This article has been accepted for publication and undergone full peer review but has not been through the copyediting, typesetting, pagination and proofreading process which may lead to differences between this version and the Version of Record. Please cite this article as doi: 10.1002/hep.32577

Footnote Page

***Corresponding Authors**:
Bin Geng *or* ***Jun Cai***, Hypertension Center, Fuwai Hospital, Chinese Academy of Medical Sciences and Peking Union Medical College, Beijing, P.R. China. E-mail: bingeng@hsc.pku.edu.cn; caijun@fuwaihospital.org;

Liming Yang, Department of Pathophysiology, Harbin Medical University-Daqing, Daqing, China. E-mail: limingyang@ems.hrbmu.edu.cn

Ming-hua Zheng, NAFLD Research Center, Department of Hepatology, the First Affiliated Hospital of Wenzhou Medical University, Wenzhou, China. E-mail: zhengmh@wmu.edu.cn

†These authors contributed equally to this work.

Abbreviation List: ACC: acetyl-CoA carboxylase; ApoC II: Apolipoprotein C II; BSEP: bile salt export pump; CARD11: caspase recruitment domain family member 11; CBS: cystathionine β synthase; CREB5: cAMP responsive element binding protein 5; CSE: cystathionine γ lyase; CYP7A1: Cholesterol 7-alpha hydroxylase; DCA: deoxycholic acid; FAS: fatty acid synthase; FXR: farnesoid X receptor; H_2S: hydrogen sulfide; HFD: high fat diet; HMGCR: HMG-CoA Reductase; ITPR2: inositol 1,4,5-trisphosphate receptor type 2; ITT: insulin tolerance test; LCA: lithocholic acid; LPL: lipoprotein lipase; LXR: liver X receptor; MAFG: v-maf musculoaponeurotic fibrosarcoma oncogene family protein G; MST: 3-mercaptopyruvate sulfur transferase; NAFLD: non-alcoholic fatty liver; NASH: non-alcoholic steatohepatitis; OGTT: oral glucose tolerance test; PID1: phosphotyrosine interaction domain containing 1; PPARs: peroxisome proliferator activated receptors; PTT: pyruvate tolerance test; SCD1: stearoyl-CoA desaturase 1; SHP: small heterodimer partner; SPP1: secreted phosphoprotein 1; SREBP: sterol regulatory element binding protein; TβMCA: tauro-β-muricholic acid; TC: total cholesterol; TG: triglycerides; TSS: transcription start sites

Financial Support: This work was supported by the National Natural Science Foundation of China (81870318, 81860111, 82100492, 81800367, 81825002, 82000835); CAMS Innovation Fund for Medical Sciences (2021-1-I2M-007); Science Research Program of Xi'an Medical University (Program No.2020DOC13); High Level Creative Talents from Department of Public Health in Zhejiang Province (S2032102600032).

Abstract

Background & Aim: Hydrogen sulfide (H_2S) plays a protective role in non-alcoholic fatty liver disease (NAFLD). However, whether cystathionine gamma lyase (CSE), a dominant H_2S generating enzyme in hepatocytes, has a role in the pathogenesis of NAFLD is currently unclear.

Approach & Results: We showed that CSE protein expression is dramatically down-regulated, especially in fibrotic areas, in livers from NAFLD patients. In high fat diet (HFD)-induced NAFLD mice, or an oleic acid-induced hepatocyte model, the CSE/H_2S pathway is also down-regulated. To illustrate a regulatory role for CSE in NAFLD, we generated a hepatocyte-specific CSE knockout mouse (CSE^{LKO}). Feeding a HFD to CSE^{LKO} mice, they showed more hepatic lipid deposition with increased activity of the fatty acid de-novo synthesis pathway, increased hepatic insulin resistance and higher hepatic gluconeogenic ability, compared to CSE^{Loxp} control mice. By contrast, H_2S donor treatment attenuated these phenotypes. Furthermore, the protection conferred by H_2S was blocked by Farnesoid X receptor (FXR) knockdown. Consistently, serum deoxycholic acid and lithocholic acid (FXR antagonists) were increased, and tauro-β-muricholic acid (FXR activation elevated) was reduced in CSE^{LKO}. CSE/H_2S promoted a novel post-translation modification (sulfhydration) of FXR at Cys138/141 sites, thereby enhancing its activity to modulate expression of target genes related to lipid and glucose metabolism, inflammation, and fibrosis. Sulfhydration proteomics in patient's liver supported the CSE/H_2S modulation noted in the CSE^{LKO} mice.

Conclusion: FXR-sulfhydration is a novel post-translational modification affected by hepatic endogenous CSE/H_2S that may promote FXR activity and attenuate NAFLD. Hepatic CSE deficiency promotes development of non-alcoholic steatohepatitis. The interaction between H_2S and FXR may be amenable to therapeutic drug treatment in NAFLD.

INTRODUCTION

Non-alcoholic fatty liver disease (NAFLD) is a common chronic liver disease characterized by lipid accumulation in hepatocytes (steatosis) with or without inflammation (non-alcoholic steatohepatitis, NASH) (1). NAFLD not only contributes to the development of cirrhosis, hepatocellular carcinoma and type 2 diabetes mellitus, but is also associated with an increased risk of developing cardiovascular events (2).

Nuclear receptors such as peroxisome proliferator activated receptors (PPARs), liver X receptor (LXR) and farnesoid X receptor (FXR) play a crucial role in the pathogenesis of NAFLD (3). Targeting nuclear receptors, such as FXR with the agonist obeticholic acid (OCA, which is approved by FDA to treat cholestatic liver diseases) may attenuate liver inflammation, steatosis and enhance insulin sensitivity (4, 5). Although this drug has some side effects, such as pruritus and increases in plasma low density lipoprotein cholesterol, OCA is a promising drug for the treatment of NASH (6).

Hydrogen sulfide (H_2S) is a novel gas transmitter that is dependent on cystathionine β synthase (CBS), cystathionine γ lyase (CSE) or 3-mercaptopyruvate sulfur transferase (3-MST) activity in the liver (7). CSE protein exceeds CBS protein by about 60-fold in mouse liver and about 90% H_2S biosynthetic activity might be sourced from CSE (8). In a high fat diet (HFD) induced NAFLD mouse model, hepatic CSE/H_2S is significantly down-regulated (9, 10). By contrast, H_2S donor lowers HFD-induced steatosis and serum triglyceride concentrations by AMPK-mTOR mediated hepatocyte autophagy (11), or by inhibition of hepatic acetyl-CoA activity (12). Furthermore, inhibition of 3-MST reduced HFD-induced NAFLD by up-regulating the CSE/H_2S pathway (13). Dietary methionine restriction or physical exercise may also attenuate HFD-induced hepatic lipid accumulation by enhancing the CSE/H_2S pathway (14, 15). More interestingly, H_2S donor modulated proliferator-activated receptor γ (PPARγ) activity in HFD mice (16), and reduced low density lipoprotein receptor independent of LXR activity (17), that may be relevant in NAFLD. Thus, these studies highlight a potential preventative role of CSE/H_2S in NAFLD, and also raise the following two main research questions: what are the relevant CSE/H_2S changes in NAFLD patients, and what is the role of hepatic endogenous CSE/H_2S regulation in NAFLD?

In the present experimental study, we have compared liver CSE expression in subjects with and without NAFLD. We then confirmed these changes in liver CSE expression both in HFD-induced NAFLD mouse liver and in oleic acid-stimulated primary mouse hepatocytes. In a hepatocyte-conditional CSE knockout mouse model, we also compared the liver lipid deposition changes involving FXR regulation.

METHODS AND MATERIALS

Patients

A total of 23 non-NAFLD individuals and 22 age- and sex-matched patients with NAFLD who had undergone liver biopsy were recruited at the First Affiliated Hospital of Wenzhou Medical University. The inclusion criteria of the study were as follows: obese patients undergoing bariatric surgery with no prior evidence of liver diseases. Liver biopsy was performed during the bariatric procedure. Exclusion criteria of the study were as follows: current excessive drinking (average daily consumption of > 20 g alcohol/day for women and > 30 g alcohol/day for men); chronic use of potential hepatotoxic drugs; viral hepatitis, or haemochromatosis (18). Written informed consent was obtained from each patient. The study protocol conformed to the ethical guidelines of the 1975 Declaration of Helsinki as reflected in a priori approval by the ethics committees of the First Affiliated Hospital of Wenzhou Medical University (NO. 2016-0246).

Animal model

Wild type mice were purchased from the Animal Center, Fuwai Hospital. $CSE^{flox/flox}$ (CSE^{Loxp}) mice (C57BL/6J background) were generated by inserting loxP sites between exon 1 and 4 of CSE genes (**Figure S1**). Liver CSE conditional knockout (CSE^{LKO}) mice were generated by hybridizing CSE^{Loxp} mouse with an albumin promoter-driven Cre recombinase transgenic mouse. Male C57BL/6J mice, CSE^{Loxp} and CSE^{LKO} mice (sibling littermates) aged 8 weeks were fed with a high fatty diet (60 kcal% fat, Research Diets D12492, USA) for 12 weeks to induce NAFLD in the animal model. A normal chow diet (Research Diets 12450J) was used as the control diet. Two H_2S donors, i.e., NaHS (50 mg/kg/day) and GYY4137 (46 mg/kg/day), or vehicle (normal saline, 0.1 ml/day) treatments were given by intraperitoneal injections.

The mice were housed under a 12-hour light/dark cycle with *ad libitum* access to food and water. All animal experiments were approved by the Ethics Committee on Animal Care of Fuwai Hospital, and the investigation complied with the animal Management Rule of the Ministry of Health, People's Republic of China (document No. 55, 2001) and Guide for the Care and Use of Laboratory Animals of the US National Institutes of Health.

Statistical analysis

Data are expressed as means and standard deviation (SD). Normality of the data distribution was checked by the Kolmogorov Smirnov test. Differences between groups were evaluated with the unpaired Students t-test. For three or more groups, data were compared by using the one-way analysis of variance (ANOVA), followed by Tukey post-hoc analysis. Comparisons including two factors were performed by two-way ANOVA. Repeated measures on the same animals were analyzed using two-way mixed-effects ANOVA. All statistical analysis involved using GraphPad Prism v8.0.2. $P<0.05$ was considered statistically significant.

NB: For other methods and material details, see the expanded Methods Section in the Online Data Supplement.

RESULTS

Down-regulation CSE/H_2S in NAFLD patients and mice

Since liver expresses CSE, CBS and 3-MST enzymes, we confirmed that CSE (5.8 fold increase compared to CBS, and 48.9 fold increase compared to 3-MST, **Figure S1B**) is the dominant H_2S generation enzymes in mouse liver tissues. We performed immunohistochemical staining for CSE and CBS in both 23 NAFLD patients (steatosis confirmed by hematoxylin-eosin (H&E) staining, **Figure S2A**) and 22 non-NAFLD individuals (see **Table S1**), who underwent liver biopsy.

In these NAFLD patient's livers, hepatic CSE expression was significantly down-regulated by about 33% compared to that in non-NAFLD patient's livers (**Figure 1A**). CBS protein was not changed (**Figure S2B**). More intriguingly, the CSE protein in the liver fibrotic area was markedly decreased (**Figure 1A**). To confirm this, we also measured the CSE/H_2S changes in HFD-induced NAFLD mouse liver. In keeping with the aforementioned changes in NAFLD patients, CSE mRNA (**Figure 1B**) and protein expression was decreased (**Figure 1C & Figure S3**) and confirmed by immunohistochemical staining (**Figure 1D**) in HFD mouse liver, without changes in CBS (**Figure S4**) and 3-MST (**Figure 1C**) expression. Coinciding with CSE down-regulation, hepatic H_2S generation was also reduced (about 33%) in HFD mice (**Figure 1E**).

To investigate whether the CSE/H_2S down-regulation was stimulated by lipid deposition, we treated primary mouse hepatocytes with oleic acid (400 μM) for 24 h. LipidTox staining showed abundant intracellular lipid droplets associated with a reduction in H_2S generation (mito-HS staining, **Figure 1F**). Accordingly, only CSE but not CBS or 3-MST protein, was decreased in oleic acid (OA)-stimulated cells (**Figure 1G**). These results suggest that hepatic lipid deposition was associated with CSE/H_2S reduction.

Hepatic CSE/H_2S attenuated HFD-induced steatosis and insulin resistance

To evaluate the role for hepatic CSE/H_2S in NAFLD, we constructed a hepatic-conditional CSE knockout mice (CSE^{LKO}) by loxp/cre recombination system (**Figure S1A**). This mouse model confirmed CSE deletion in hepatocytes by CSE mRNA and protein expression (**Figure S1C**), and there was a ~75% decrease in H_2S generation in liver tissues (**Figure S1D**). Because the CSE global knockout caused hyperhomocysteinemia, we also measured serum homocysteine and cysteine levels, and confirmed that hepatocyte specific deletion of CSE did not induce CBS mRNA expression (**Figure S5A),** or cause hyperhomocysteinemia, but lowered cysteine synthesis (**Figure S1E**). Feeding a HFD for 12 weeks, the CSE^{LKO} mice developed more severe hepatic steatosis compared to control mice (CSE^{Loxp}) (**Figure 2A**). H&E

and Sirius Red staining showed hepatocyte ballooning with Mallory-Denk bodies, lobular inflammation, and heightened collagen fiber in CSE^{LKO} liver (**Figure 2B**), thus indicating that these mice are prone to developing NASH. In line with hepatic lipid deposition, serum and liver triglyceride (TG) levels and serum total cholesterol (TC) levels were increased in CSE^{LKO} mice (**Figure 2C**). Oral glucose tolerance tests (OGTT, **Figure 2D**), intravenous insulin tolerance tests (ITT, **Figure 2E**), and pyruvate tolerance tests (PTT, **Figure 2F**) in CSE^{LKO} mice indicated that CSE deficiency exacerbated both glucose homeostasis and insulin resistance.

To investigate the major pathophysiological processes in CSE/H_2S on liver lipid metabolism, we screened the essential regulatory genes, including fatty acid de novo synthesis, triglyceride synthesis, fatty acid oxidation and fatty acid uptake by qRT-PCR. As shown in **Figure 2G**, most regulated genes were fatty acid de novo synthetic genes in CSE^{LKO} liver. These genes coding proteins (sterol response element binding protein 1c (SREBP-1c), acetyl-CoA carboxylase (ACC), fatty acid synthase (FAS), stearoyl-CoA desaturase 1 (SCD1)) were also increased in CSE^{LKO} mice (**Figure 2H and Figure S5B**). In primary hepatocytes, CSE deficiency also increased lipid droplets, which were reversed by NaHS supplementation (**Figure S6**). These loss of function experiments indicate that hepatic CSE deletion exacerbated HFD-induced steatosis and insulin resistance, in part via enhancing fatty acid de novo synthesis; and increased risk of NASH.

In contrast, we treated HFD-induced NAFLD mice with two H_2S donors: NaHS (50 mg/kg/day) and GYY4137 (46 mg/kg/day) by intraperitoneal injections. HFD model mice received equal volumes of normal saline injection. After treating for 12 weeks, H_2S donors dramatically attenuated HFD-induced steatosis, by H&E (**Figure 3A**) and oil red O staining (**Figure 3B**) analysis. H_2S donor treatment also lowered serum and liver triglyceride levels, and liver cholesterol levels (**Figure 3C**). OGTT (**Figure 3D**), ITT (**Figure 3E**) and PTT (**Figure 3F**) data showed down-regulation of fatty acid de novo synthesis-associated genes: SREBP-1c, ACC, FAS, and SCD1. Protein expression was also lowered after H_2S donor treatment (**Figure 3G&H**). Therefore, the loss of function and donor's treatment experiments highlighted hepatic CSE/H_2S protection in NAFLD.

CSE/H_2S attenuated steatosis by FXR

To further clarify the possible molecular mechanism(s) of CSE/H_2S protection in steatosis development, we performed liver transcriptome analysis in both CSE^{LKO} and CSE^{LOXP} mice. Here, we identified 151 up-regulated and 561 down-regulated genes, and the heatmap graph is shown in **Figure S7A**, and the Volcano Plot in **Figure 4A**. GO enrichment genes included cholesterol, sterol, lipid, fatty acid metabolism and biosynthesis pathway (**Figure 4B**). By STRING function protein association network analysis, we focused on an essential metabolic nuclear receptor-farnesoid X receptor (FXR, Nr1h4 gene) in NAFLD (**Figure S7B**). Liver FXR protein expression was markedly reduced in CSE^{LKO} mice (**Figure 4C**), but it was up-regulated after NaHS treatment (**Figure 4D**). Consistently, knockdown CSE decreased, and overexpression

of CSE increased FXR mRNA (**Figure 4E**) and protein levels (**Figure 4F & Figure S8A**). H_2S donor treatment of primary hepatocytes also increased FXR protein expression (**Figure S8B**). In line with FXR expression and activation, some essential genes involved in fatty acid de novo synthesis: SREBP-1c, ACC, FAS, and SCD1 mRNA (**Figure 4G**) and protein (**Figure 4H**) expression also showed inverted changes associated with CSE knockdown or overexpression.

To confirm a role for FXR in CSE/H_2S protection, we designed and identified a small interference RNA of FXR (**Figure S9A**). We then constructed and purified the knockdown-FXR lentivirus, which effectively lowered the FXR protein level (**Figure S9B**) in primary mouse hepatocytes. By scrambled RNA-GFP control lentivirus transfection into hepatocytes (**Figure S9C**), we counted the multiplicity of infection (MOI) of the virus. Next, we injected control lentivirus (10 MOI) by tail vein, and confirmed the transfection efficiency *in vivo* (**Figure S9D**). Using lentivirus knockdown hepatic FXR, more severe hepatic steatosis developed with HFD-induction, and which abolished the protective effect of the H_2S donor on steatosis (**Figure 5A**). In addition, knockdown FXR also blocked the H_2S protection on triglyceride, cholesterol and glucose metabolism (**Figure 5B**); OGTT (**Figure 5C**), ITT (**Figure 5D**) and PTT (**Figure 5E**), respectively. For mechanism, H_2S-attenuated fatty acid de novo synthesis (Figure 5F&G) also blocked, while FXR-knockdown. We also measured the FXR target genes-HMG-CoA reductase (HMGCR), apolipoprotein C II (ApoC II), small heterodimer partner (SHP), v-maf musculoaponeurotic fibrosarcoma oncogene family protein-G (MAFG), cholesterol 7-alpha hydroxylase (CYP7A1) and lipoprotein lipase (LPL) expression in liver tissues, and confirmed activation FXR by H_2S treatment (**Figure S10**).

By contrast, the FXR target genes-SHP, MAFG, BSEP were down-regulated, and CYP7A1 was up-regulated in the liver of CSE^{LKO} mice compared to that observed in CSE^{LOXP} mice (**Figure S11**). Because FXR is a bile acid metabolism-related receptor, we measured serum bile acid compositions. As **Figure S12A** shows, the serum bile composition was different between CSE^{LKO} and CSE^{LOXP} mice. Interestingly, serum FXR antagonistic bile acids-LCA and DCA were increased, (similar to NAFLD patients (19)); whereas TβMCA (increased by FXR agonist (20)) was decreased in CSE^{LKO} mice (**Figure S12A&B**). These results indicate that hepatic CSE/H_2S may ameliorate steatosis in part via FXR activation.

CSE/H_2S sulfhydrates FXR to increase Zn^{2+} binding and promote FXR activity

FXR is a zinc finger protein that has two conserved C4 zinc fingers in its DNA binding domain (**Figure S13**). Zinc binding protein such as sirtin-1 could be sulfhydrated by H_2S and activating its de-acetylation activity (21). Therefore, we investigated whether the sulfhydration of FXR affects its activity. Treatment with NaHS caused FXR sulfhydration as identified in vitro (mouse liver tissues homogenate; **Figure 6A**) and in vivo (primary mouse hepatocytes; **Figure 6B**). Knockdown of CSE decreased (**Figure 6C**), and by contrast overexpression of CSE increased FXR sulfhydration (**Figure 6D**). In keeping with changes in cellular FXR sulfhydration, sulfhydrated FXR in CSE^{LKO}

liver tissues was dramatically decreased in comparison to that of CSE^{LOXP}. FXR sulfhydration was also reduced in NAFLD mice liver tissues, and was rescued by the H_2S donors (NaHS or GYY) (**Figure 6D**). In patients, we confirmed FXR sulfhydration in two non-NAFLD patients' liver samples, but no one in NAFLD patients (**Figure S14A).** These results highlight that FXR could be sulfhydrated by CSE/H_2S, that in turn down-regulates lipid deposition.

To investigate protein sulfhydration in NAFLD development, we measured the sulfhydrated-proteomics of patients. Using biotin-switch assays, we identified 160 sulfhydrated proteins in five NAFLD patients' liver tissues, and 246 proteins in five non-NAFLD patients. There were 106 proteins that overlapped between the two patient groups. Metascape Gene Ontology (GO) networks analysis showed that overlapped gene were enriched for fatty acid metabolism, moncarboxylic acid metabolism, sulfur amino acid metabolism, ROS and protein folding (**Figure S14B**). This proteomics analysis indicates CSE/H_2S determines protein sulfhydration including FXR and may play an important role in NASH.

To elucidate whether FXR sulfhydration was associated with its transcription activity, we first detected FXR nuclear translocation. As **Figure 6E** & **Figure S15A** indicate, sulfhydated FXR mediated by NaHS significantly increased nuclear translocation. Conversely, removing FXR sulfhydration with DTT reduced nuclear translocation. Correspondingly, fatty acid synthesis related genes (SREPB-1c, FAS and ACC), cholesterol synthesis genes (HMGCR) and CYP7A1 were down-regulated with FXR sulfhydration, and were up-regulated after removing sulfhydration (**Figure 6F**). ChIP-qPCR data also confirmed that sulfhydration enhanced FXR binding to BSEP promoter, and de-sulfhydration lowered it (**Figure 6G & Figure S15B**). Consistent with these data, sulfhydration increased FXR and Zn^{2+} binding, whereas de-sulfhydration decreased it (**Figure 6H&I**). These data indicate that CSE/H_2S sulfhydrates FXR and increased its binding to Zn^{2+}, thereby promoting its nuclear translocation, DNA binding activity and transcription regulation.

Because there were two conserved Zn^{2+} binding domains in FXR, we next identified the sulfhydration sites by mutation of major cysteine residue sites. We constructed five mutation plasmids targeting four CXXC domain as shown as **Figure S13**. We co-expressed FXR/FXR mutation, RXR, BSEP promoter luciferase report plasmids in 293-HEK cells, then demonstrated that all five mutations lowered FXR interaction with the BSEP promoter (**Figure S16A**), suggesting that Zn^{2+} binding is essential for FXR activity. By biotin-switch assays, Cys138/141 double mutation and all 8 cysteine residue sites mutation, dramatically reduced FXR sulfhydration (**Figure 7A, Figure S16B),** suggesting Cys138/141 of FXR as a major sulfhydration site. In line with sulfhydration lowering, H_2S-promoted FXR nuclear translocation was reduced in M1 and M1-4 mutations (**Figure 7B & Figure S16C**). FXR-sulfhydration regulated-fatty acid de-novo synthesis related genes (SREBP-1c, FAS and ACC) expression (**Figure 7C**), binding to Zn^{2+} (**Figure 7D&E**), and BSEP promoter binding activity (**Figure 7F, Figure S16D)** were also blocked by M1 and M1-4 mutation. Co-IP assay also showed

M1 mutation reduced FXR interaction with the RXR protein (**Figure 7G**). For functional analysis, treating 293-HEK cells with oleic acid (200 μM) and NaHS (100 μM) for 12 h, showed that the Cys138/141mutation blocked H_2S-activated FXR target genes-SHP, MAFG, and BSEP mRNA expression (**Figure S17**). Taken together, these data confirmed that the Cys138/141 sites are the major sulfhydration sites and regulation sites of H_2S-promoting FXR activity.

FXR sulfhydration modulated lipid and glucose metabolism, fibrosis, and inflammation-related genes

Above data demonstrate that FXR sulfhydration at Cys138/141 sites promote its transcription activity. Therefore, whether FXR sulfhydration occupied genes take part in the pathogenesis of NAFLD was investigated. We performed ChIP-Seq in CSE deleted hepatocytes or Cys138/141S mutation of HEK-293 cells. By clustering FXR occupied peaks within ± 3.0 kb from the center of transcription start sites (TSS), inhibiting sulfhydration (CSE knockout) slightly increased, and removing sulfhydration (Cys138/141S mutation) mildly decreased, FXR occupancy genes compared with the wild type (**Figure. 8A**). By cross-analysis we identified 1374 up-regulated and 700 down-regulated genes in Cys139/141S mutation-enrichment genes; and 212 up-regulated and 189 down-regulated genes in CSE knockout-enrichment genes. We then performed bulk RNA-sequencing, and identified 251 Cys139/141S mutation-enrichment genes by intersection between Chip-seq changed and RNA-seq changed genes, and 16 CSE-KO enriched genes (**Figure 8B**). GO analysis showed that these genes were enriched for fatty acid and cholesterol metabolism, insulin signalling and glucose metabolism, immunity and inflammation, and in the fibrosis pathway (**Figure 8C**). Amongst these genes, we used integrative genomics viewer screenshots to exhibit some selected genes-CREB5, PID1, ITPR2, SPP1, CARD11, and then confirmed that reducing (CSE KO) or removing (Cys138/141S mutation) sulfhydration FXR decreased binding to the promoter of these genes (**Figure 8D**). These high output experiments confirm CSE/H_2S protection by sulfhydrating FXR; thereby attenuating hepatic lipid deposition, insulin resistance, inflammation, and liver fibrosis.

DISCUSSION

CBS and CSE are two key enzymes in the methionine trans-sulfuration pathway, and function as a single system in mammalian cysteine generation and concomitant H_2S production (22). H_2S exhibits a protective role in high fatty diet-induced NAFLD (9, 11) or a methionine-choline deficient diet that induces NASH (23). These data infer that hepatic CSE might play an essential role in NAFLD development, due to the dominant expression of CSE in liver compared to CBS (8).

In the present study, we confirmed hepatocellular CSE expression was down-regulated in NAFLD patients, HFD-induced fatty liver mice and oleic acid-treated hepatocytes. Hepatocyte specific deletion of CSE exacerbated HFD-induced lipid deposition in hepatocytes, and the affected livers were prone to NASH with fibrosis. In contrast, H_2S donor treatment attenuated these effects of decreased CSE activity. Next, we demonstrated that FXR sulfhydration in its zinc finger domain by the CSE/H_2S system, effected a novel translational modification that promoted FXR activity. In turn, FXR-activation could up-regulate CSE expression (24), and this interaction between FXR and CSE increased hepatic protection in NAFLD (**Figure S18**).

Many studies have addressed the effects of endogenous H_2S generation system changes in the pathogenesis of NAFLD. According to a previous study, CBS and CSE expression is up-regulated in HFD-induced mice after 5 weeks exposure (25). In contrast, in another study, it was demonstrated that CSE protein was significantly reduced in the liver of mice fed a HFD for more than 8 weeks, and this was associated with a compensatory increase in CBS protein (9). It has also been shown that expression of another H_2S generating enzyme in the liver (3-MST) is also increased both in patients with NAFLD and in a HFD mouse model (13). Here, we first confirmed that CSE protein levels were decreased in the steatotic liver tissues in NAFLD patients. Consistently, CSE protein expression is also down-regulated in the liver tissues of mice fed a HFD for 12 weeks; or in oleic acid-treated hepatocytes. However, we did not find that CBS or 3-MST was increased neither in our mouse model nor in our cell model. Collectively, these data suggest that hepatic CSE expression is up-regulated in the early stages of NAFLD, possibly due to compensatory changes induced by oxidative stress (25), or local inflammation with increased tumor necrosis factor-α (26) (TNFα has been shown to quickly induce CSE expression (27)). In cirrhosis phase, CSE protein was markedly decreased and was almost undetectable in the areas of fibrosis (**Figure1A**).

It has been previously shown that in the CBS knockout mouse liver there were enlarged multi-nucleated hepatocytes filled with microvesicular lipid droplets (28), hepatic oxidative stress, perilobular mononuclear inflammatory infiltration and pericellular fibrosis (29), and also hyperhomocysteinemia (28, 29) (i.e., a non-invasive marker of NAFLD(30)). In contrast to that model, global CSE deletion did not induce any indices of hepatic dysfunction and was associated with mildly elevated serum homocysteine levels, and H_2S production reduction (31). A global knockout of CBS and CSE induced methionine metabolism and caused hyperhomocysteinemia. To clarify the role of endogenous CSE in the pathogenesis of NAFLD, we used a hepatocyte specific CSE

knockout mouse (CSE^{LKO}) model, which decreased by ~75% the generation ability of H_2S, but did not increase serum homocysteine levels. Feeding these CSE^{LKO} mice with a HFD for 12 weeks, more severe hepatic steatosis, insulin resistance and increased serum lipids occurred, with more marked de novo fatty acid synthesis (coinciding with H_2S donor inhibitory effects(23)). However, there were no significant increases in fatty acid uptake, oxidation, or triglyceride synthesis. More interestingly, CSE^{LKO} mice showed an increase in lobular inflammation infiltration and collagen deposition, suggesting a potential risk to development of NASH with fibrosis. Global CSE knockout mice also developed severe hepatic steatosis with higher serum cholesterol and lower serum/liver triglyceride levels, in association with LXRα down-regulation (32). Although there was a similar steatosis phenotype between the global CSE knockout and our model, the intestinal CSE loss may also disturb fatty acid and bile acid absorption, which may cause the differences in triglyceride levels and LXRα expression in these two mouse models. Therefore, the present study provides more precise evidence of the distinct role of the hepatocellular endogenous CSE/H_2S system in the pathogenesis of NAFLD.

FXR is an essential metabolic nuclear receptor affecting cholesterol secretion, bile acid biosynthesis, glucose and lipid metabolism (33). The FXR agonists-obeticholic acid (34, 35) and cilofexor (36) have reduced hepatic fat content in phase 2 and 3 randomized clinical trials. FXR activation affects its target genes such as small heterodimer partner (SHP) and FGF19 expression and modulates fatty acid de novo synthesis (37), FAS (38), fatty acid oxidation (39), VLDL secretion (40) and triglyceride clearance (by increasing apoC-II and decreasing apoC-III, ANGPTL, to enhance LPL activity) (33). Here, by screening RNA-seq data and by enrichment analysis, we identified and confirmed that FXR levels were prone to CSE changes by genomic modification. By contrast, the effect of H_2S donor protection in NAFLD (in accord with previous studies (11, 41)) was blocked by knockdown of FXR, thus indicating that the FXR pathway may be a novel molecular mechanism of H_2S hepatocellular protection. Due to FXR activation, H_2S lowered fatty acid de novo synthesis genes, such as SREBP1c, FAS(41), ACC and SCD1; triglyceride clearance genes, such as apoC-II upregulation, apoC-III and LPL reduction. Therefore, this study is the first to show that CSE/H_2S system is a potential activator of FXR.

FXR activity is also mediated by post-translational modification. FXR agonist promote FXR Ser154 phosphorylation, modulating its activity, and subsequent degradation (42). Phosphorylation at Tyr67 site increases FXR activity contributing to bile acid synthesis (43). Methylation at Lys 206 site increases FXR transcription activity (44). Acetylation at Lys 217 enhances its stability but inhibits its binding activity to RXR (45). The Lys-122 and Lys-277 sites of FXR can be SUMOylated, and Lys-277 SUMOylation regulates FXR trans-repression of inflammatory gene expression (46). Atypical SUMOylation at Lys-325 which requires prior Ser-327 phosphorylation also contributes to FXR activity and its degradation (47). Here, we have identified a new post-translational modification, sulfhydration of FXR at Cys138/141 sites. This post-translational modification promotes FXR binding to Zn^{2+}, FXR nuclear translocation,

and target genes transcription. Therefore, we propose that sulfhydration of FXR is a novel post translation of FXR, affecting its transcriptional activity.

Bile acids receptors G protein-coupled bile acid receptor 1 (GPBAR1, also known as TGR5) (48), and FXR activation increase CSE expression/activity and H_2S production (24). Experimental evidence also demonstrates that CSE is a target gene of FXR (24). Here, our data shows that CSE/H_2S may sulfhydrate FXR at a Zn^{2+} binding domian and promote its transcriptional ability. More intriguingly, Chip-seq association with RNA-seq cross-analysis showed that FXR sufhydration was associated with changes in genes affecting lipid metabolism, inflammation, fibrosis and glucose metabolic regulation. Thus, hepatic CSE/H_2S and FXR interaction highlights a novel "positive feedback mechanism" affecting bile acid metabolism, hepatic steatosis and fibrosis.

Both clinical trials and animal experiments demonstrated that FXR agonist such as OCA or some small molecular chemicals, effectively reduced NAFLD, but increased potential risk of pruritus or cardiovascular diseases (serum cholesterol elevation). H_2S per se exerts anti-inflammation, anti-fibrosis and immunoregulatory effects, and also lowered serum cholesterol and anti-atherosclerosis. Futhurmore, H_2S enhanced FXR activity, then heightened CSE/H_2S by "positive feedback" regulation, to make up CSE/H_2S system reduction in NAFLD. Thus FXR agonist combination with H_2S donor, or FXR agonist-derived H_2S donors to treat NAFLD, one maybe reduce FXR agonist dose, the other H_2S per se cardiovascular protection effects, could be effective for attenuate NAFLD or NASH, meanwhile avoid side-effects of FXR agonists.

Acknowledgements
We would like to thank Professor Ming-Hua Zheng and Dr. Yu Han for providing non-NAFLD and NAFLD patients liver biopsy samples; Liming Yang for providing condition CSE knockout construction with alb-cre mice.

Contributors
BG and JC conceived the idea and designed the experiments. WX, CC, ZC, and HZ performed experiments. CC and QC performed the bioinformatic analysis. MHZ, JF and GX analyzed the data and improved the manuscript. CB and GT critically reviewed the data and contributed to writing the manuscript.

Competing interests
None declared.

References

1. Younossi ZM, Koenig AB, Abdelatif D, Fazel Y, Henry L, Wymer M. Global epidemiology of nonalcoholic fatty liver disease-Meta-analytic assessment of prevalence, incidence, and outcomes. Hepatology 2016;64:73-84.

2. Lombardi R, Iuculano F, Pallini G, Fargion S, Fracanzani AL. Nutrients, Genetic Factors, and Their Interaction in Non-Alcoholic Fatty Liver Disease and Cardiovascular Disease. Int J Mol Sci 2020;21.

3. Cave MC, Clair HB, Hardesty JE, Falkner KC, Feng W, Clark BJ, Sidey J, et al. Nuclear receptors and nonalcoholic fatty liver disease. Biochim Biophys Acta 2016;1859:1083-1099.

4. Cruz-Ramón V, Chinchilla-López P, Ramírez-Pérez O, Méndez-Sánchez N. Bile Acids in Nonalcoholic Fatty Liver Disease: New Concepts and therapeutic advances. Ann Hepatol 2017;16:s58-s67.

5. Mudaliar S, Henry RR, Sanyal AJ, Morrow L, Marschall HU, Kipnes M, Adorini L, et al. Efficacy and safety of the farnesoid X receptor agonist obeticholic acid in patients with type 2 diabetes and nonalcoholic fatty liver disease. Gastroenterology 2013;145:574-582 e571.

6. Rau M, Geier A. An update on drug development for the treatment of nonalcoholic fatty liver disease - from ongoing clinical trials to future therapy. Expert Rev Clin Pharmacol 2021;14:333-340.

7. Wang R. Physiological implications of hydrogen sulfide: a whiff exploration that blossomed. Physiol Rev 2012;92:791-896.

8. Singh S, Banerjee R. PLP-dependent H(2)S biogenesis. Biochim Biophys Acta 2011;1814:1518-1527.

9. Peh MT, Anwar AB, Ng DS, Atan MS, Kumar SD, Moore PK. Effect of feeding a high fat diet on hydrogen sulfide (H2S) metabolism in the mouse. Nitric Oxide 2014;41:138-145.

10. Bravo E, Palleschi S, Aspichueta P, Buque X, Rossi B, Cano A, Napolitano M, et al. High fat diet-induced non alcoholic fatty liver disease in rats is associated with hyperhomocysteinemia caused by down regulation of the transsulphuration pathway. Lipids Health Dis 2011;10:60.

11. Sun L, Zhang S, Yu C, Pan Z, Liu Y, Zhao J, Wang X, et al. Hydrogen sulfide reduces serum triglyceride by activating liver autophagy via the AMPK-mTOR pathway. Am J Physiol Endocrinol Metab 2015;309:E925-935.

12. Ali A, Zhang Y, Fu M, Pei Y, Wu L, Wang R, Yang G. Cystathionine gamma-lyase/H(2)S system suppresses hepatic acetyl-CoA accumulation and nonalcoholic fatty liver disease in mice. Life Sci 2020;252:117661.

13. Li M, Xu C, Shi J, Ding J, Wan X, Chen D, Gao J, et al. Fatty acids promote fatty liver disease via the dysregulation of 3-mercaptopyruvate sulfurtransferase/hydrogen sulfide pathway. Gut 2018;67:2169-2180.

14. Wang B, Zeng J, Gu Q. Exercise restores bioavailability of hydrogen sulfide and promotes autophagy influx in livers of mice fed with high-fat diet. Can J Physiol Pharmacol 2017;95:667-674.

15. Yang Y, Wang Y, Sun J, Zhang J, Guo H, Shi Y, Cheng X, et al. Dietary methionine restriction reduces hepatic steatosis and oxidative stress in high-fat-fed mice by promoting H(2)S production. Food Funct 2019;10:61-77.

16. Cai J, Shi X, Wang H, Fan J, Feng Y, Lin X, Yang J, et al. Cystathionine gamma lyase-

hydrogen sulfide increases peroxisome proliferator-activated receptor gamma activity by sulfhydration at C139 site thereby promoting glucose uptake and lipid storage in adipocytes. Biochim Biophys Acta 2016;1861:419-429.
17. Huang Y, Ning K, Li WW, Lin G, Hou CL, Wang MJ, Zhu YC. Hydrogen sulfide accumulates LDL receptor precursor via downregulating PCSK9 in HepG2 cells. Am J Physiol Cell Physiol 2020;319:C1082-C1096.
18. Liu B, Xiang L, Ji J, Liu W, Chen Y, Xia M, Liu Y, et al. Sparcl1 promotes nonalcoholic steatohepatitis progression in mice through upregulation of CCL2. J Clin Invest 2021;131:e144801.
19. Jiao N, Baker SS, Chapa-Rodriguez A, Liu W, Nugent CA, Tsompana M, Mastrandrea L, et al. Suppressed hepatic bile acid signalling despite elevated production of primary and secondary bile acids in NAFLD. Gut 2018;67:1881-1891.
20. Clifford BL, Sedgeman LR, Williams KJ, Morand P, Cheng A, Jarrett KE, Chan AP, et al. FXR activation protects against NAFLD via bile-acid-dependent reductions in lipid absorption. Cell Metab 2021;33:1671-1684.e1674.
21. Du C, Lin X, Xu W, Zheng F, Cai J, Yang J, Cui Q, et al. Sulfhydrated Sirtuin-1 Increasing Its Deacetylation Activity Is an Essential Epigenetics Mechanism of Anti-Atherogenesis by Hydrogen Sulfide. Antioxid Redox Signal 2019;30:184-197.
22. Sarna LK, Siow YL, O K. The CBS/CSE system: a potential therapeutic target in NAFLD? Can J Physiol Pharmacol 2015;93:1-11.
23. Luo ZL, Tang LJ, Wang T, Dai RW, Ren JD, Cheng L, Xiang K, et al. Effects of treatment with hydrogen sulfide on methionine-choline deficient diet-induced non-alcoholic steatohepatitis in rats. J Gastroenterol Hepatol 2014;29:215-222.
24. Renga B, Mencarelli A, Migliorati M, Distrutti E, Fiorucci S. Bile-acid-activated farnesoid X receptor regulates hydrogen sulfide production and hepatic microcirculation. World J Gastroenterol 2009;15:2097-2108.
25. Hwang SY, Sarna LK, Siow YL, O K. High-fat diet stimulates hepatic cystathionine β-synthase and cystathionine γ-lyase expression. Can J Physiol Pharmacol 2013;91:913-919.
26. Cobbina E, Akhlaghi F. Non-alcoholic fatty liver disease (NAFLD) - pathogenesis, classification, and effect on drug metabolizing enzymes and transporters. Drug Metab Rev 2017;49:197-211.
27. Perkins ND. Cysteine 38 holds the key to NF-kappaB activation. Mol Cell 2012;45:1-3.
28. Watanabe M, Osada J, Aratani Y, Kluckman K, Reddick R, Malinow MR, Maeda N. Mice deficient in cystathionine beta-synthase: animal models for mild and severe homocyst(e)inemia. Proc Natl Acad Sci U S A 1995;92:1585-1589.
29. Robert K, Nehme J, Bourdon E, Pivert G, Friguet B, Delcayre C, Delabar JM, et al. Cystathionine beta synthase deficiency promotes oxidative stress, fibrosis, and steatosis in mice liver. Gastroenterology 2005;128:1405-1415.
30. Polyzos SA, Kountouras J, Patsiaoura K, Katsiki E, Zafeiriadou E, Deretzi G, Zavos C, et al. Serum homocysteine levels in patients with nonalcoholic fatty liver disease. Ann Hepatol 2012;11:68-76.
31. Mani S, Yang G, Wang R. A critical life-supporting role for cystathionine gamma-lyase in the absence of dietary cysteine supply. Free Radic Biol Med 2011;50:1280-1287.
32. Mani S, Li H, Yang G, Wu L, Wang R. Deficiency of cystathionine gamma-lyase and

hepatic cholesterol accumulation during mouse fatty liver development. Science Bulletin 2015;60:336-347.
33. Lefebvre P, Cariou B, Lien F, Kuipers F, Staels B. Role of bile acids and bile acid receptors in metabolic regulation. Physiol Rev 2009;89:147-191.
34. Neuschwander-Tetri BA, Loomba R, Sanyal AJ, Lavine JE, Van Natta ML, Abdelmalek MF, Chalasani N, et al. Farnesoid X nuclear receptor ligand obeticholic acid for non-cirrhotic, non-alcoholic steatohepatitis (FLINT): a multicentre, randomised, placebo-controlled trial. Lancet 2015;385:956-965.
35. Younossi ZM, Ratziu V, Loomba R, Rinella M, Anstee QM, Goodman Z, Bedossa P, et al. Obeticholic acid for the treatment of non-alcoholic steatohepatitis: interim analysis from a multicentre, randomised, placebo-controlled phase 3 trial. Lancet 2019;394:2184-2196.
36. Patel K, Harrison SA, Elkhashab M, Trotter JF, Herring R, Rojter SE, Kayali Z, et al. Cilofexor, a Nonsteroidal FXR Agonist, in Patients With Noncirrhotic NASH: A Phase 2 Randomized Controlled Trial. Hepatology 2020;72:58-71.
37. Watanabe M, Houten SM, Wang L, Moschetta A, Mangelsdorf DJ, Heyman RA, Moore DD, et al. Bile acids lower triglyceride levels via a pathway involving FXR, SHP, and SREBP-1c. J Clin Invest 2004;113:1408-1418.
38. Matsukuma KE, Bennett MK, Huang J, Wang L, Gil G, Osborne TF. Coordinated control of bile acids and lipogenesis through FXR-dependent regulation of fatty acid synthase. J Lipid Res 2006;47:2754-2761.
39. Pineda Torra I, Claudel T, Duval C, Kosykh V, Fruchart JC, Staels B. Bile acids induce the expression of the human peroxisome proliferator-activated receptor alpha gene via activation of the farnesoid X receptor. Mol Endocrinol 2003;17:259-272.
40. Hirokane H, Nakahara M, Tachibana S, Shimizu M, Sato R. Bile acid reduces the secretion of very low density lipoprotein by repressing microsomal triglyceride transfer protein gene expression mediated by hepatocyte nuclear factor-4. J Biol Chem 2004;279:45685-45692.
41. Wu D, Zheng N, Qi K, Cheng H, Sun Z, Gao B, Zhang Y, et al. Exogenous hydrogen sulfide mitigates the fatty liver in obese mice through improving lipid metabolism and antioxidant potential. Med Gas Res 2015;5:1.
42. Hashiguchi T, Arakawa S, Takahashi S, Gonzalez FJ, Sueyoshi T, Negishi M. Phosphorylation of Farnesoid X Receptor at Serine 154 Links Ligand Activation With Degradation. Mol Endocrinol 2016;30:1070-1080.
43. Byun S, Kim DH, Ryerson D, Kim YC, Sun H, Kong B, Yau P, et al. Postprandial FGF19-induced phosphorylation by Src is critical for FXR function in bile acid homeostasis. Nat Commun 2018;9:2590.
44. Balasubramaniyan N, Ananthanarayanan M, Suchy FJ. Direct methylation of FXR by Set7/9, a lysine methyltransferase, regulates the expression of FXR target genes. Am J Physiol Gastrointest Liver Physiol 2012;302:G937-947.
45. Kemper JK, Xiao Z, Ponugoti B, Miao J, Fang S, Kanamaluru D, Tsang S, et al. FXR acetylation is normally dynamically regulated by p300 and SIRT1 but constitutively elevated in metabolic disease states. Cell Metab 2009;10:392-404.
46. Kim DH, Xiao Z, Kwon S, Sun X, Ryerson D, Tkac D, Ma P, et al. A dysregulated acetyl/SUMO switch of FXR promotes hepatic inflammation in obesity. EMBO J 2015;34:184-199.

47. Bilodeau S, Caron V, Gagnon J, Kuftedjian A, Tremblay A. A CK2-RNF4 interplay coordinates non-canonical SUMOylation and degradation of nuclear receptor FXR. J Mol Cell Biol 2017;9:195-208.
48. Renga B, Bucci M, Cipriani S, Carino A, Monti MC, Zampella A, Gargiulo A, et al. Cystathionine γ-lyase, a H2S-generating enzyme, is a GPBAR1-regulated gene and contributes to vasodilation caused by secondary bile acids. Am J Physiol Heart Circ Physiol 2015;309:H114-126.

Figure Legends

Figure 1 Down-regulation of hepatic CSE/H_2S in NAFLD patients and mice. (A) Immunohistochemistry (IHC) staining of CSE in liver biopsy from NAFLD and non-NAFLD patients. Protein expression was evaluated by a H-score semiquantitative approach. Bar=20 μm. Red line area is a fibrotic area. There is no positive CSE staining in this area. (B) Endogenous H_2S generation key enzymes: CBS, CSE and 3-MST mRNA expression, protein expression by western blot (C) or IHC staining, Bar=20 μm (D) in HFD-induced NAFLD mice. N=5. (E) H_2S generation ratio of mouse liver tissue was measured by methylene blue assay. N=7-8. (F) Oleic acid (400 μM, OA) treated primary mouse hepatocytes for 48 h, LipidTox staining for lipid deposition, Mito-HS for H_2S production. (G) CBS, CSE and 3-MST protein expression were measured in OA treated hepatocytes. N=6.

Figure 2 Hepatic CSE deletion mice exacerbated HFD-induced NAFLD. (A) General pathology (Bar=1 cm), and Oil Red O staining (Bar=50 μm) for liver tissues in hepatic CSE specific knockout mice (CSE^{LKO}) and control loxp/loxp mice (CSE^{Loxp}). (B) H&E and Sirius red staining for liver tissues. Bar=50 μm. (C) Serum triglyceride (TG) and total cholesterol (TC) levels; (C) liver TG and TC level in NAFLD mice. (D) Oral glucose tolerance test (OGTT), (E) Insulin tolerance test (ITT), (F) Pyruvate tolerance test (PTT) was compared between CSE^{LKO} and CSE^{Loxp}. N=8-10 in all animal experiments. (G) Lipid metabolism related genes expression was assayed by qRT-PCR. N=6. ** P<0.01. (F) Fatty acid de novo synthesis related protein's expression was detected by western blot. N=6.

Figure 3 H_2S donor treatment ameliorated HDF-induced NAFLD and glucose metabolism disorder. In HDF-induced NAFLD mouse model, H_2S donor-NaHS or GYY4137 treatment for 12 weeks, then H&E staining (A), Oil Red O staining (B) was used for evaluation the lipid deposition in liver. Bar=50 μm. (C) Changes of serum TG, TC; and liver TG, TC level after H_2S donor treatment. * P<0.05; ** P<0.01. (D) OGTT, (E) ITT and (F) PTT changes after H_2S donor's treatment. Two-way mixed effect ANOVA was used, ** P<0.01 vs normal chow, # P<0.05 vs HFD. (G) Fatty acid de novo synthesis related protein expression by western blot. (H) The semi-quantitative analysis of above proteins by relative gray density plus area of target protein comparison to β-actin. ** P<0.01. 6 independent experiments were performed.

Figure 4 Hepatocellular endogenous CSE/H_2S up-regulated FXR expression. Total RNA was extracted from about 30 mg liver tissue of CSE^{LKO} or CSE^{Loxp} mice, then bulk RNA-sequencing was performed. (A) Volcano plot showed the down-regulated genes (blue) and up-regulated genes (Red) in CSE^{LKO} compared with CSE^{Loxp} mice. Hollow point presented the GO-enriched genes. (B) GO-analysis showed the changed genes enrichment the major pathway. (C) FXR protein expression in CSE knockout liver tissues. N=6. (D) Hepatic FXR protein level changes after H_2S donor treatment. Overexpression CSE by adenovirus, or knockdown CSE by siRNA in hepG2 cells, the FXR mRNA (E), and protein expression (F) changes. N=6. Then, the fatty acid de novo synthesis related genes: SREBP1-c, ACC, FAS, and SCD mRNA (N=4) (G) and protein expression (H) changes associated with CSE overexpression or knockdown. * P<0.05; ** P<0.01. N=6.

Figure 5 Knockdown FXR by lentivirus blocked H_2S donor's protection on NAFLD. Knockdown FXR shRNA lentivirus (10 MOI) was bolus injected by tail vein before HFD feeding. Continue feeding HFD for 12 weeks, the H&E staining for liver tissue morphology, Oil Red O staining for hepatic lipid deposition. Bar=100 μm (A). (B) Serum and liver TG, TC level were measured. * P<0.05, ** P<0.01. (C) OGTT, (D) ITT and (E) PTT was assayed for glucose metabolism. * P<0.05, ** P<0.01. N=8 in this animal experiment. (F) Hepatic FXR protein, fatty acid de novo synthesis genes: SREBP1-c, ACC, FAS and SCD protein expression was detected by western blot. N=6. (G) The semi-quantitative analysis of above protein. * P<0.05, ** P<0.01.

Figure 6 CSE/H_2S sulfhydrated FXR and promoted its binding to Zn^{2+} then enhancing its activity. (A) Biotin switch assay for FXR sulfhydration in vitro. (B) HepG2 cells were treated with NaHS or DTT, then the FXR immunoprecipitation using antibody, then biotin switch assay was performed for FXR sulfhydration in vivo. N=5. (C) Knockdown or overexpressed CSE, intracellular FXR sulfhydration level changes. N=3. (D) Alterations of hepatic FXR sulfhydration in animal model, including in CSE^{LKO} and CSE^{Loxp}, H_2S donor's treatment model and FXR knockdown model. N=4-6. (E) Nuclear FXR translocation was detected whilst FXR sulfhydration by NaHS or removing sulfhydration by DTT. N=6. (F) FXR sulfhydration dependent transcription activity was evaluated by FXR associated or target genes expression. N=8. (G) ChIP-qPCR identified the FXR binding activity to BSEP (a famous FXR target gene) promoter whilst FXR sulfhydration or de-sulfhydration. N=6. (H) Using His-tagged and Ni column system to purify FXR, then 1μg FXR incubation with NaHS or DTT, Zn^{2+} and Zn^{2+}-probe for 30 min, after washing, the FXR-Zn^{2+} binding was detected by fluorescence density count. N=6. (I) In vivo FXR-Zn2+ binding was showed by co-fluorescence of FXR (Red) and Zn^{2+} probe (blue), as white arrow pointed. In this figure, * P<0.05, ** P<0.01.

Figure 7 Identify the FXR sulfhydration sites. Mutation 4 zinc finger areas named M1, M2, M3, M4, or and all mutation (M1-4) of FXR, then transfected these plasmids into 293-HEK cells. (A) The changes of FXR sulfhydration while mutation different sites. N=5. (B) The different mutation effect on FXR nuclear translocation. N=5. (C) These mutations on H_2S-mediated SREBP1-c, ACC, and FAS mRNA expression. Mutation different sites on H_2S-mediated FXR-Zn^{2+} binding activity in vitro (D), or in vivo (E). N=6. H_2S regulated FXR binding to promoter of BESP by ChIP-qPCR (F). (G) Co-IP assay for FXR and RXR interaction while H2S donor treatment in FXR or M1 transfected cells. In this figure, * P<0.05, ** P<0.01. N=6.

Figure 8 Sulfhydrated FXR mediated lipid and glucose metabolism, inflammation, fibrosis genes. ChIP-seq was performed while reduced FXR sulfhydration (CSE knockout hepatocytes) or removed FXR sulfhydration (Cys138/141 sites mutation plasmid transfected 293-HEK cells). (A) Heat map of FXR-occupied genes based on FXR signal around FXR peak center. (B) Volcano plot showed the FXR-occupied genes while removed (mutation) or reduced (knockout) sulfhydration (upper panel), cross-analysis the bulk RNA-seq data then the overlapped genes were shown by Venn diagram. (C) Gene Ontology (GO) analysis in mutation or knockout enriched genes. (D) Visualization of ChIP-Seq results for five representative FXR sulfhydration occupied genes (lipid and glucose correlated: CREB5, PID1, IPTR; fibrosis correlated: SPP1;

inflammation correlated: CARD11) by Integrative Genomics Viewer (IGV). N=4.

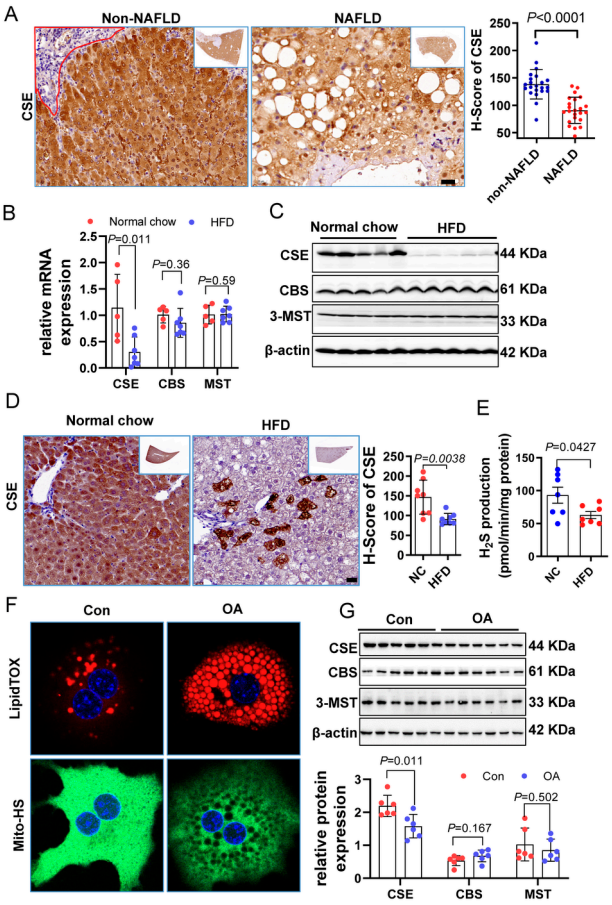

HEP_32577_Figure 1.tiff

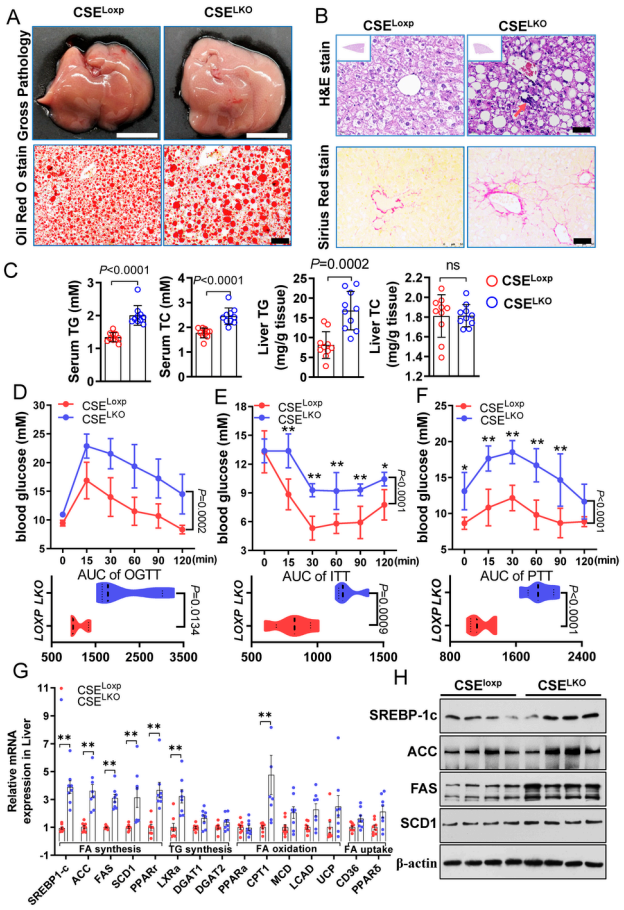

HEP_32577_Figure 2.tiff

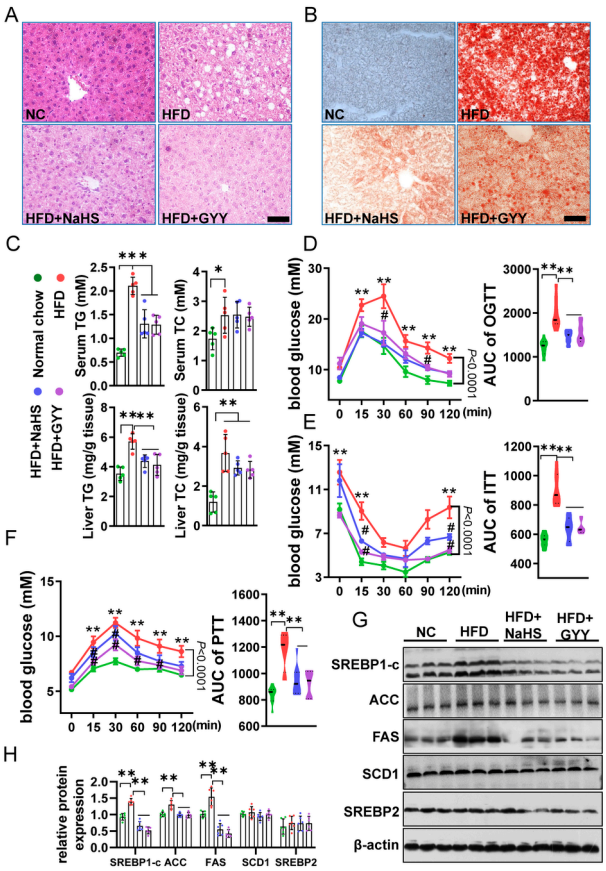

HEP_32577_Figure 3.tiff

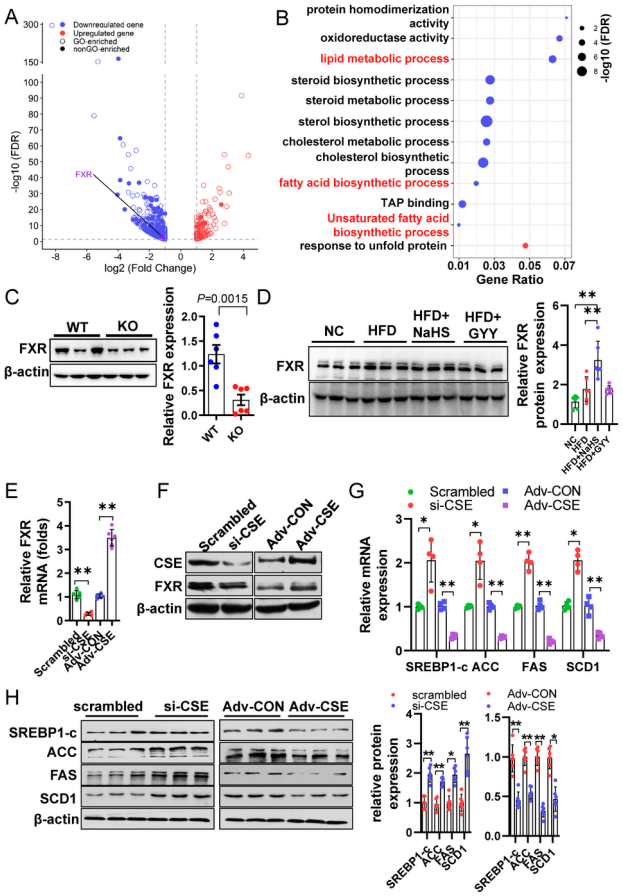

HEP_32577_Figure 4.tiff

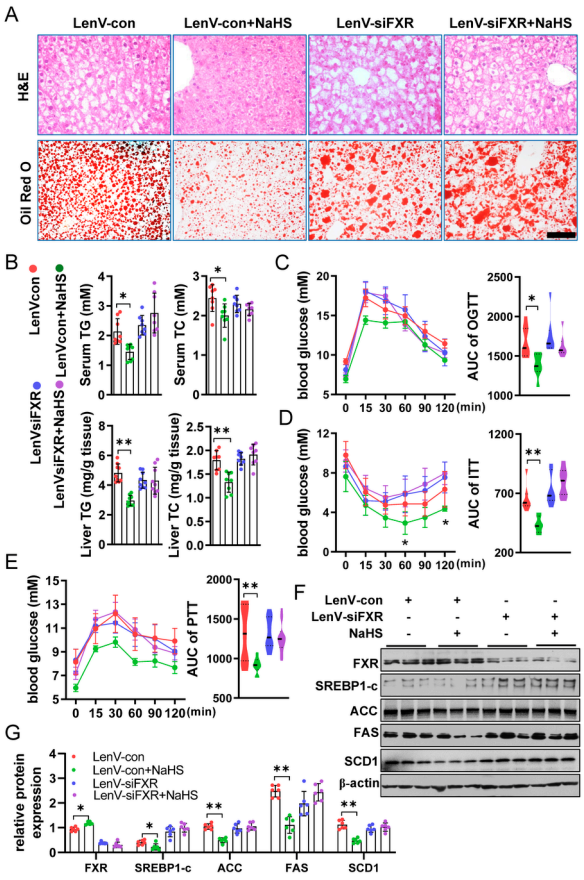

HEP_32577_Figure 5.tiff

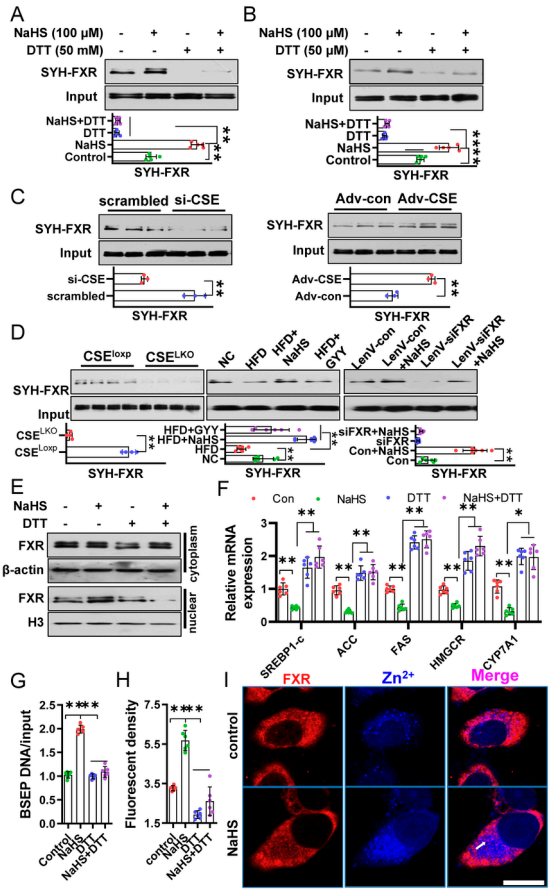

HEP_32577_Figure 6.tiff

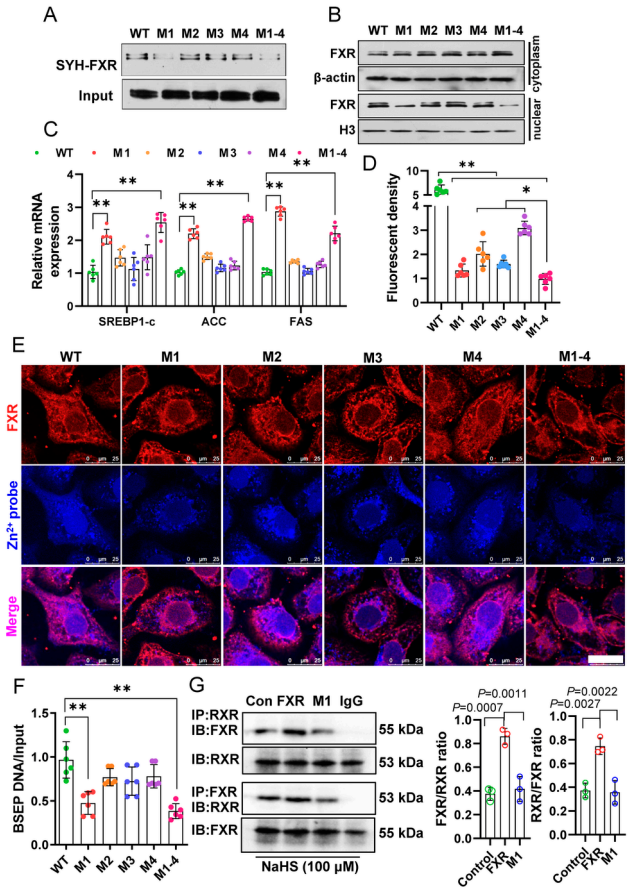

HEP_32577_Figure 7.tiff

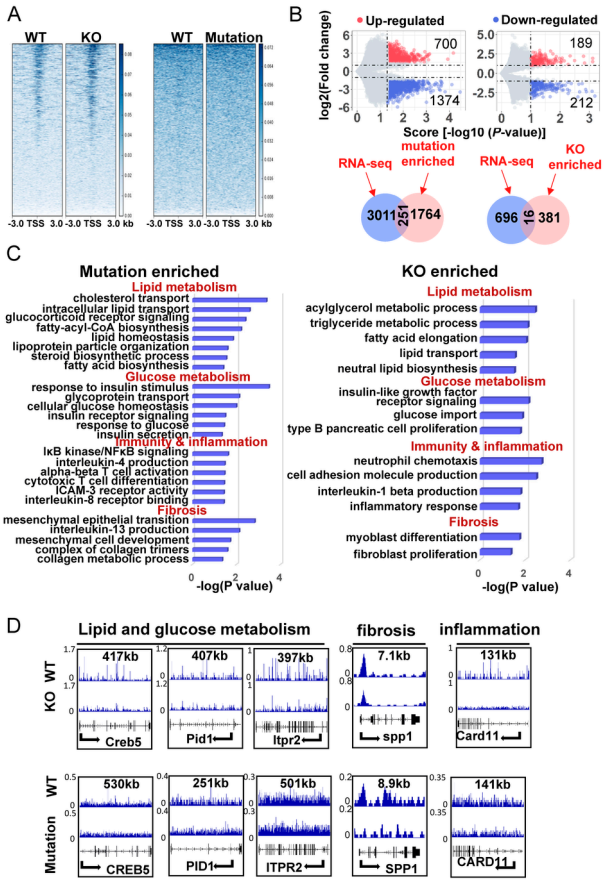

HEP_32577_Figure 8.tiff